Tracing the source of nitrate in a forested stream showing elevated concentrations during storm events

Weitian Ding[1], Urumu Tsunogai[1], Fumiko Nakagawa[1], Takashi Sambuichi[1], Hiroyuki Sase[2], Masayuki Morohashi[2], Hiroki Yotsuyanagi[2]

[1] Graduate School of Environmental Studies, Nagoya University, Furo-cho, Chikusa-ku, Nagoya 464-8601, Japan

[2] Asia Center for Air Pollution Research, 1182 Sowa, Nishi-ku, Niigata-shi, Niigata 950-2144, Japan

Corresponding author: Weitian Ding, Email: ding.weitian.v2@s.mail.nagoya-u.ac.jp

1   **Abstract**

2   To clarify the source of nitrate increased during storm events in a temperate forested

3   stream, we monitored temporal variation in the concentrations and stable isotopic

4   compositions including $\Delta^{17}O$ of stream nitrate in a forested catchment (KJ catchment,

5   Japan) during three storm events I, II, and III (summer). The stream showed significant

6   increase in nitrate concentration, from 24.7 µM to 122.6 µM, from 28.7 µM to 134.1

7   µM, and from 46.6 µM to 114.5 µM during the storm events I, II, and III, respectively.

8   On the other hand, the isotopic compositions ($\delta^{15}N$, $\delta^{18}O$, and $\Delta^{17}O$) of stream nitrate

9   showed a decrease in accordance with the increase in the stream nitrate concentration,

10   from +2.5 ‰ to −0.1 ‰, from +3.0 ‰ to −0.5 ‰, and from +3.5 ‰ to −0.1 ‰ for $\delta^{15}N$,

11   from +3.1 ‰ to −3.4 ‰, from +2.9 ‰ to −2.5 ‰, and from +2.1 ‰ to −2.3 ‰ for $\delta^{18}O$,

12   and from +1.6 ‰ to +0.3 ‰, from +1.4 ‰ to +0.3 ‰, and from +1.2 ‰ to +0.5 ‰ for

13   $\Delta^{17}O$ during the storm events I, II, and III, respectively. Besides, we found strong linear

14   relationships between the isotopic compositions of stream nitrate and the reciprocal of

15   stream nitrate concentrations during each storm event, implying that the temporal

16   variation in the stream nitrate can be explained by simple mixing between two

17   distinctive endmembers of nitrate having different isotopic compositions. Furthermore,

18   we found that both concentrations and the isotopic compositions of soil nitrate obtained

19   in the riparian zone of the stream were plotted on the nitrate-enriched extension of the

20   linear relationship. We conclude that the soil nitrate in the riparian zone was primarily

21   responsible for the increase in stream nitrate during the storm events. In addition, we

found that the concentration of unprocessed atmospheric nitrate in the stream was stable at 1.6 ± 0.4 µM, 1.8 ± 0.4 µM, and 2.1 ± 0.4 µM during the storm events I, II, and III, respectively, irrespective to the significant variations in the total nitrate concentration. We conclude that the storm events have little impacts on the concentration of unprocessed atmospheric nitrate in the stream and thus the annual export flux of unprocessed atmospheric nitrate relative to the annual deposition flux can be a robust index to evaluate nitrogen saturation in forested catchments, irrespective to the variation in the number of storm events and/or the variation in the elapsed time from storm events to sampling.

1 Introduction

Nitrate is an important nitrogenous nutrient in biosphere. Traditionally, forested ecosystems have been considered nitrogen limited (Vitousek and Howarth, 1991). Due to the elevated loading of nitrogen through atmospheric deposition, however, some forested ecosystems become nitrogen saturated (Aber et al., 1989), from which elevated levels of nitrate are exported (Mitchell et al., 1997; Peterjohn et al., 1996). In addition, sudden increase in the concentration of nitrate in response to storm events has been reported in forested streams worldwide (Aguilera and Melack, 2018; Creed et al., 1996; Kamisako et al., 2008; McHale et al., 2002), which further enhanced nitrate export from forested ecosystems.

Such excessive leaching of nitrate from forested catchment degrades water quality

3

43 and cause eutrophication in downstream areas (Galloway et al., 2003; Paerl and

44 Huisman, 2009). Thus, tracing the source of nitrate increase during storm events in

45 forested streams is important for sustainable forest management, especially for the

46 nitrogen-saturated forested ecosystems.

47 As for the source of nitrate that was added to stream during storm events, either of

48 the two possible sources have been assumed in past studies; (1) atmospheric nitrate

49 ($NO_3^-{}_{atm}$) in rainwater originally and being supplied directly to stream water (Inamdar

50 and Mitchell, 2006), and (2) soil nitrate originally and being supplied to stream water

51 by the flushing effects on soils (Creed et al., 1996; Ocampo et al., 2006). Nevertheless,

52 monitoring the variation in nitrate concentration, it is difficult to clarify the primary

53 source of nitrate that increases during storm events.

54 The natural stable isotopic composition of nitrate has been widely applied to clarify

55 the sources of nitrate in natural freshwater systems (Burns and Kendall, 2002; Durka et

56 al., 1994; Kendall et al., 2007). In particular, triple oxygen isotopic compositions of

57 nitrate ($\Delta^{17}O$) have been used in recent days as a conservative tracer of $NO_3^-{}_{atm}$

58 deposited onto a forested catchment (Inoue et al., 2021; Michalski et al., 2004;

59 Nakagawa et al., 2018; Tsunogai et al., 2014), showing distinctively different $\Delta^{17}O$ from

60 that of remineralized nitrate ($NO_3^-{}_{re}$), derived from organic nitrogen through general

61 chemical reactions, including microbial N mineralization and microbial nitrification.

62 While $NO_3^-{}_{re}$, the oxygen atoms of which are derived from either terrestrial O_2 or H_2O

63 through microbial processing (i.e., nitrification), always shows the relation close to the

64   "mass-dependent" relative relation between $^{17}O/^{16}O$ ratios and $^{18}O/^{16}O$ ratios; $NO_3^-{}_{atm}$

65   displays an anomalous enrichment in ^{17}O reflecting oxygen atom transfers from

66   atmospheric ozone (O_3) during the conversion of NO_X to $NO_3^-{}_{atm}$ (Alexander et al.,

67   2009; Michalski et al., 2003; Morin et al., 2011; Nelson et al., 2018). As a result, the

68     $\Delta^{17}O$ signature defined by the following equation (Kaiser et al., 2007) enables us to

69   distinguish $NO_3^-{}_{atm}$ ($\Delta^{17}O > 0$) from $NO_3^-{}_{re}$ ($\Delta^{17}O = 0$):

70
$$\Delta^{17}O = \frac{1+\delta^{17}O}{(1+\delta^{18}O)^{\beta}} - 1 \tag{1}$$

71   where the constant β is 0.5279 (Kaiser et al., 2007), $\delta^{18}O = R_{sample}/R_{standard} - 1$ and R is

72   the $^{18}O/^{16}O$ ratio (or the $^{17}O/^{16}O$ ratio in the case of $\delta^{17}O$ or the $^{15}N/^{14}N$ ratio in the case

73   of $\delta^{15}N$) of the sample and each standard reference material. In addition, $\Delta^{17}O$ is almost

74   stable during "mass-dependent" isotope fractionation processes within terrestrial

75   ecosystems. Therefore, while the $\delta^{15}N$ or $\delta^{18}O$ signature of $NO_3^-{}_{atm}$ can be overprinted

76   by the biological processes subsequent to deposition, $\Delta^{17}O$ can be used as a robust tracer

77   of unprocessed $NO_3^-{}_{atm}$ to reflect its accurate mole fraction within total NO_3^-, regardless

78   of the progress of the partial metabolism (partial removal of nitrate through

79   denitrification and assimilation) subsequent to deposition (Michalski et al., 2004;

80   Nakagawa et al., 2013, 2018; Tsunogai et al., 2011, 2014, 2018).

81   While the variation in the $\delta^{18}O$ and/or $\Delta^{17}O$ of nitrate in forested streams during storm

82   events have been reported in past studies (Sebestyen et al., 2019; Sabo et al., 2016;

83   Buda and Dewalle. 2009), the temporal resolutions of sampling were less than 10

84   times/day during storm events and the source of the stream nitrate increased during

85   storm events has not been clarified yet. In this study, we determined the temporal

86   variation in the concentrations and the isotopic compositions ($\delta^{15}N$, $\delta^{18}O$, and $\Delta^{17}O$) of

87   stream nitrate at once every hour during storm events in a forested catchment to clarify

88   (1) the source of nitrate in a forested stream that was added during storm events, and

89   (2) the temporal variation in the concentration of $NO_3^-{}_{atm}$ in response to storm events.

90   In addition, the impacts of storm events on the index of nitrogen saturation lately

91   proposed by Nakagawa et al. (2018) were discussed.

92

93   **2 Methods**

94   2.1 Study site

95   As for the studying field to trace the source of stream nitrate during storm events, we

96   chose Kajikawa forested catchment (KJ catchment) in Japan, in which several past

97   studies had been done to clarify the temporal variation in the concentration of stream

98   nitrate and the status of nitrogen saturation (Kamisako et al., 2008; Nakagawa et al.,

99   2018; Sase et al., 2021). This is a small, forested catchment (3.84 ha) located in the

100   northern part of Shibata City, Niigata Prefecture, along the coast of Sea of Japan (Fig.

101   1a). The KJ catchment predominantly slopes towards the west-northwest, with a mean

102   slope of 36°, and the elevation ranges from 60 to 170 m above sea level (Fig. 1b). The

103   catchment is fully covered by Japanese cedars (*Cryptomeria japonica* D. Don) that were

104   approximately 46 years old in 2018 (Sase et al., 2021). The parent material is

105   granodiorite and brown forest soils (Cambisols) have developed in this area (Kamisako

106   et al., 2008; Sase et al., 2008). The lowest, highest, and mean monthly temperatures

107   recorded at the nearest meteorological station (Nakajo station) were 1.0 °C (in February),

108   27.9 °C (in August), and 14.5 °C, respectively, from 2017/5 to 2020/3. The annual mean

109   precipitation was around 2500 mm, approximately 17% of which occurred during

110   spring (from March to May), approximately 20% during summer (from June to August),

111   approximately 28% during fall (from September to November), and approximately 35%

112   during winter (from December to February). The catchment usually experiences

113   snowfall from late December to March.

114   From 2003 to 2005, Kamisako et al. (2008) determined temporal variation in the

115   concentration of Ca^{2+}, Mg^{2+}, Cl^-, and NO_3^- eluted from the catchment via a stream at

116   intervals of 1 to 3 hour for 2 to 3 days on each and found that significant increase in the

117   stream nitrate concentration during storm events, from less than 30 μM to more than

118   120 μM. On the basis of the observed nitrate enrichment in the stream water, they

119   concluded that atmospheric nitrogen inputs exceeded the biological demand at the

120   catchment and proposed that the KJ catchment was under nitrogen saturation.

121   Nakagawa et al. (2018) determined temporal variation in the concentrations and stable

122   isotopic compositions ($\delta^{15}N$, $\delta^{18}O$, and $\Delta^{17}O$) of both stream nitrate and soil nitrate for

123   two years (from 2012/12 to 2014/12) and concluded that nitrate in the groundwater of

124   the catchment was the major source of nitrate in the stream water during the base flow

125   periods. Additionally, Nakagawa et al. (2018), who proposed the export flux of $NO_3^-{}_{atm}$

126   (M_{atm}) relative to the deposition flux of $NO_3^-{}_{atm}$ (D_{atm}) can be an alternative, more robust

7

127   index for nitrogen saturation in temperate forested catchments, clarified that the

128   M_{atm}/D_{atm} ratio in the KJ catchment was larger (9.4 %) than the other catchments they

129   studied simultaneously (6.5 % and 2.6 %), which also implied the KJ catchment was

130   under the nitrogen saturation. Moreover, Sase et al. (2021) reported the

131   nitrate concentration of the stream has been increasing in recent years, which implies

132   that nitrogen saturation is still ongoing in the forest.

133
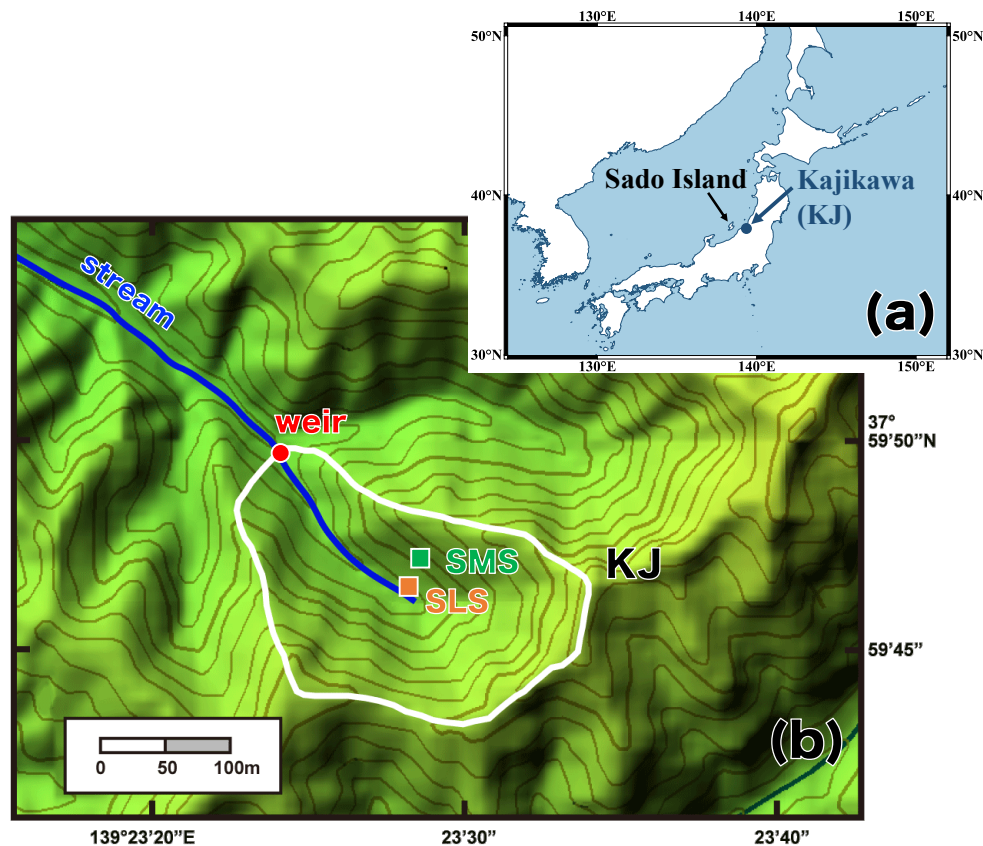
134   **Figure. 1** A map showing the locations of the studied Kajikawa (KJ) catchment in Japan

135   (a) and a colored altitude map of the KJ catchment (b) (modified after Nakagawa et al.

136   2018). The white line denotes the whole catchment area, and the red circle denotes the

137   position of the weir where the stream water was sampled. The orange (SLS) and green

138   (SMS) squares denote the sampling stations of soil water in the riparian and upland

139   zone, respectively, in the past study (Nakagawa et al., 2018).

140

141   2.2 Discharge rates and weather information

142   A V-notch weir (half angle: 30°) and a partial flume were installed at the bottom of

143   the catchment (Fig. 1b), where the discharge rates were determined. The weather

144   information including the precipitation monitored by Japan Meteorological Agency at

145   the nearest station of KJ catchment (Nakajo station; 38°04'60" N, 139°23'30" E) was

146   used for that in the KJ catchment. Because the accumulated snow was not monitored

147   in Nakajo station, however, those monitored at the Niigata station (37°53'60" N,

148   139°01'10" E) was used instead.

149

150   2.3 Sampling

151   In this study, the concentrations and stable isotopic compositions ($\delta^{15}N$, $\delta^{18}O$, and

152    $\Delta^{17}O$) of stream nitrate eluted from the KJ catchment were monitored every month for

153   more than 2 years (routine observation). Additionally, during storm events, the same

154   parameters were monitored every hour for 1 day (intensive observation). Stream water

155   was sampled at the weir located on the outlet of the KJ catchment (Fig. 1b). Routine

156   observation was performed manually using bottles at the weir approximately once a

157   month from 2017/5 to 2020/3. Intensive observation was conducted during the three

158   storm events I, II, and III (2019/8/22, 2019/10/12, and 2020/9/13, respectively), where

159   the water samples were collected at intervals of 1 hour over 24 hours using an automatic

160 water sampler (SIGMA 900, Hach, USA). In this study, 0.5 or 2 L polyethylene bottles

161 washed using chemical detergents were rinsed at least three times using deionized water

162 and dried in the laboratory before being used to store the water samples.

163

164 2.4 Analysis

165 Samples of stream water for the routine observation were transported to the

166 laboratory within 1 hour after being collected manually. Samples for the intensive

167 observation were transported within 12 days after completion of the automatic sampling

168 (Table 1). All samples were passed through a membrane filter (pore size 0.45 μm) and

169 stored in a refrigerator (4°C) until their chemical analysis.

170 The concentrations of nitrate were measured by ion chromatography (DX-500;

171 Dionex Inc., USA). To determine the stable isotopic compositions of nitrate in the

172 stream water samples, nitrate in each sample was chemically converted to N_2O using a

173 method originally developed to determine the $^{15}N/^{14}N$ and $^{18}O/^{16}O$ ratios of seawater

174 and freshwater nitrate (McIlvin and Altabet, 2005) that was later modified (Konno et

175 al., 2010; Tsunogai et al., 2011; Yamazaki et al., 2011). In brief, 11 mL of each sample

176 solution was pipetted into a vial with a septum cap. Then, 0.5 g of spongy cadmium

177 was added, followed by 150 μL of a 1 M $NaHCO_3$ solution. The sample was then shaken

178 for 18-24 h at a rate of 2 cycles s^{-1}. Then, the sample solution (10 mL) was decanted

179 into a different vial with a septum cap. After purging the solution using high-purity

180 helium, 0.4 mL of an azide–acetic acid buffer, which had also been purged using high-

181   purity helium, was added. After 45 min, the solution was alkalinized by adding 0.2 mL

182   of 6 M NaOH.

183   Then, the stable isotopic compositions ($\delta^{15}N$, $\delta^{18}O$, and $\Delta^{17}O$) of the N_2O in each vial

184   were determined using the continuous-flow isotope ratio mass spectrometry (CF-IRMS)

185   system at Nagoya University. The analytical procedures performed using the CF-IRMS

186   system were the same as those detailed in previous studies (Hirota et al., 2010; Komatsu

187   et al., 2008). The obtained values of $\delta^{15}N$, $\delta^{18}O$, and $\Delta^{17}O$ for the N_2O derived from the

188   nitrate in each sample were compared with those derived from our local laboratory

189   nitrate standards to calibrate the values of the sample nitrate to an international scale

190   and to correct for both isotope fractionation during the chemical conversion to N_2O and

191   the progress of oxygen isotope exchange between the nitrate derived reaction

192   intermediate and water (ca. 20 %). The local laboratory nitrate standards used for the

193   calibration had been calibrated using the internationally distributed isotope reference

194   materials (USGS-34 and USGS-35). In this study, we adopted the internal standard

195   method (Nakagawa et al., 2013, 2018; Tsunogai et al., 2014) to calibrate the stable

196   isotopic compositions of sample nitrate. In order to calibrate the differences in $\delta^{18}O$ of

197   H_2O between the samples and those our local laboratory nitrate standards were added

198   for calibration, the $\delta^{18}O$ values of H_2O in the samples were analyzed as well (Tsunogai

199   et al., 2010, 2011, 2014).

200   To determine whether the conversion rate from nitrate to N_2O was sufficient, the

201   concentration of nitrate in the samples was determined each time we analyzed the

202   isotopic composition using CF-IRMS based on the N_2O^+ or O_2^+ outputs. We adopted

203   the $\delta^{15}N$, $\delta^{18}O$, and $\Delta^{17}O$ values only when the concentration measured via CF-IRMS

204   correlated with the concentration measured via ion chromatography prior to isotope

205   analysis within a difference of 10 %.

206   Three kinds of the local laboratory nitrate standards were used to determine the

207   isotopic compositions of stream nitrate, which had been named to be GG01 ($\delta^{15}N = -$

208   3.07 ‰, $\delta^{18}O = +1.10$ ‰, and $\Delta^{17}O = 0$ ‰), HDLW02 ($\delta^{15}N = +16.11$ ‰, $\delta^{18}O = +22.$

209   20 ‰), and NF ($\delta^{18}O = +54.14$ ‰, $\Delta^{17}O = +19.16$ ‰). Both GG01 and HDLW02 were

210   used to determine $\delta^{15}N$ and $\delta^{18}O$ of stream nitrate, and both GG01 and NF were used

211   to determine $\Delta^{17}O$ of stream nitrate. The standard errors of the mean in the isotopic

212   compositions ($\delta^{15}N$, $\delta^{18}O$, and $\Delta^{17}O$) determined through repeated measurements on

213   GG01 (n = 3), were ±0.17 ‰ for $\delta^{15}N$, ±0.25 ‰ for $\delta^{18}O$, and ±0.10 ‰ for $\Delta^{17}O$, during

214   the measurements in this study. We repeated the analysis of $\delta^{15}N$, $\delta^{18}O$, and $\Delta^{17}O$ values

215   for each sample at least three times to attain high precision. All samples had a nitrate

216   concentration of greater than 10 μM, which corresponded to a nitrate quantity greater

217   than 100 nmol in a 10 mL sample. Thus, all isotope values presented in this study have

218   an error (standard error of the mean) better than ±0.2 ‰ for $\delta^{15}N$, ±0.3 ‰ for $\delta^{18}O$, and

219   ±0.1 ‰ for $\Delta^{17}O$.

220   Nitrite (NO_2^-) in the samples interferes with the final N_2O produced from nitrate

221   because the chemical method also converts NO_2^- to N_2O (McIlvin and Altabet, 2005).

222   Therefore, it is sometimes necessary to remove NO_2^- prior to converting nitrate to N_2O.

223 However, in this study, all the stream and soil water samples analyzed for stable isotopic

224 composition had NO_2^- concentrations lower than the detection limit (0.05 µM).

225 Because the minimum nitrate concentration in the samples was 24.7 µM in this study,

226 the ratios of NO_2^- to nitrate in the samples must be less than 0.2 %. Thus, we skipped

227 the processes for removing NO_2^-.

228

229 2.5 Calculating of the concentration of unprocessed $NO_{3\ atm}^-$ in stream water

230 The $\Delta^{17}O$ data of nitrate in each sample can be used to estimate the concentration of

231 $NO_{3\ atm}^-$ ($[NO_{3\ atm}^-]$) in the stream water samples by applying Eq. (2):

232 $$[NO_{3\ atm}^-]/[NO_3^-] = \Delta^{17}O/\Delta^{17}O_{atm} \tag{2}$$

233 where $[NO_{3\ atm}^-]$ and $[NO_3^-]$ denote the concentration of $NO_{3\ atm}^-$ and nitrate (total) in

234 each water sample, respectively, and $\Delta^{17}O_{atm}$ and $\Delta^{17}O$ denote the $\Delta^{17}O$ values of

235 $NO_{3\ atm}^-$ and nitrate (total) in the stream water sample, respectively. In this study, we

236 used the average $\Delta^{17}O$ value of $NO_{3\ atm}^-$ determined at the nearby Sado-Seki monitoring

237 station during the observation from April 2009 to March 2012 ($\Delta^{17}O_{atm} = +26.3$ ‰;

238 Tsunogai et al., 2016) for $\Delta^{17}O_{atm}$ in Eq. (2) to estimate $[NO_{3\ atm}^-]$ in the stream. We

239 allow for an error range in of 3 ‰ in $\Delta^{17}O_{atm}$, in which the factor changes in $\Delta^{17}O_{atm}$

240 from +26.3 ‰ caused by both areal and seasonal variation in the $\Delta^{17}O$ values of $NO_{3\ atm}^-$

241 have been considered (Nakagawa et al., 2018; Tsunogai et al., 2016).

242

243

244 **Table 1.** Information on the samples taken during the intensive observation.

| Storm event	Start time	End time	Date of filtration	Maximum period of storage without filtration
I	2019/8/22 16:00	2019/8/23 15:00	2019/8/29	7 days
II	2019/10/12 15:00	2019/10/13 14:00	2019/10/23	11 days
III	2020/9/13 11:00	2020/9/14 10:00	2020/9/25	12 days

245

246 **3 Results**

247 3.1 Variation during the routine observation

248   During the routine observation, the concentrations of stream nitrate ranged from

249 35.7 μM to 129.3 μM with the flux-weighted average concentration of 55.6 μM (Fig.

250 2a), showing little temporal changes from that determined during the past observations

251 from 2013 to 2014 at the same catchment (58.4 μM; Nakagawa et al., 2018). The

252 variation range also agreed with the past observation done in the same catchment

253 (Kamisako et al., 2008), except for the extraordinarily large concentration (129.3 μM)

254 recorded on 2018/8/31, which exceeded the 2σ of the whole variation range of stream

255 nitrate of our routine observation (Fig. 2a). We will discuss the reason in section 4.2.

256   The stable isotopic compositions of stream nitrate during the routine observation

257 ranged from +0.1 ‰ to +5.9‰ for $\delta^{15}N$ (Fig. 2b), from −1.9 ‰ to +7.7 ‰ for $\delta^{18}O$ (Fig.

258 2c), and from +0.4 ‰ to +2.7 ‰ for $\Delta^{17}O$ (Fig. 2d), while showing little seasonal

259 variation. The flux-weighted averages for the $\delta^{15}N$, $\delta^{18}O$, and $\Delta^{17}O$ values of nitrate

260 were +2.0 ‰, +1.1 ‰, and +1.1 ‰, respectively. Except for the extraordinarily large

261 $\delta^{18}O$ and $\Delta^{17}O$ values we found on 2019/1/31 ($\delta^{18}O$ = +7.7 ‰ and $\Delta^{17}O$ = +2.7 ‰)

262   (Figs. 2c and 2d), the values are typical for stream nitrate eluted from temperate forested

263   catchments (Hattori et al., 2019; Huang et al., 2020; Nakagawa et al., 2013, 2018; Riha

264   et al., 2014; Sabo et al., 2016; Tsunogai et al., 2014, 2016). On the other hand, the data

265   recorded on 2019/1/31 exceeded the 2σ variation range of the whole $\delta^{18}O$ and $\Delta^{17}O$

266   data. We will discuss the reason in section 4.3.

267
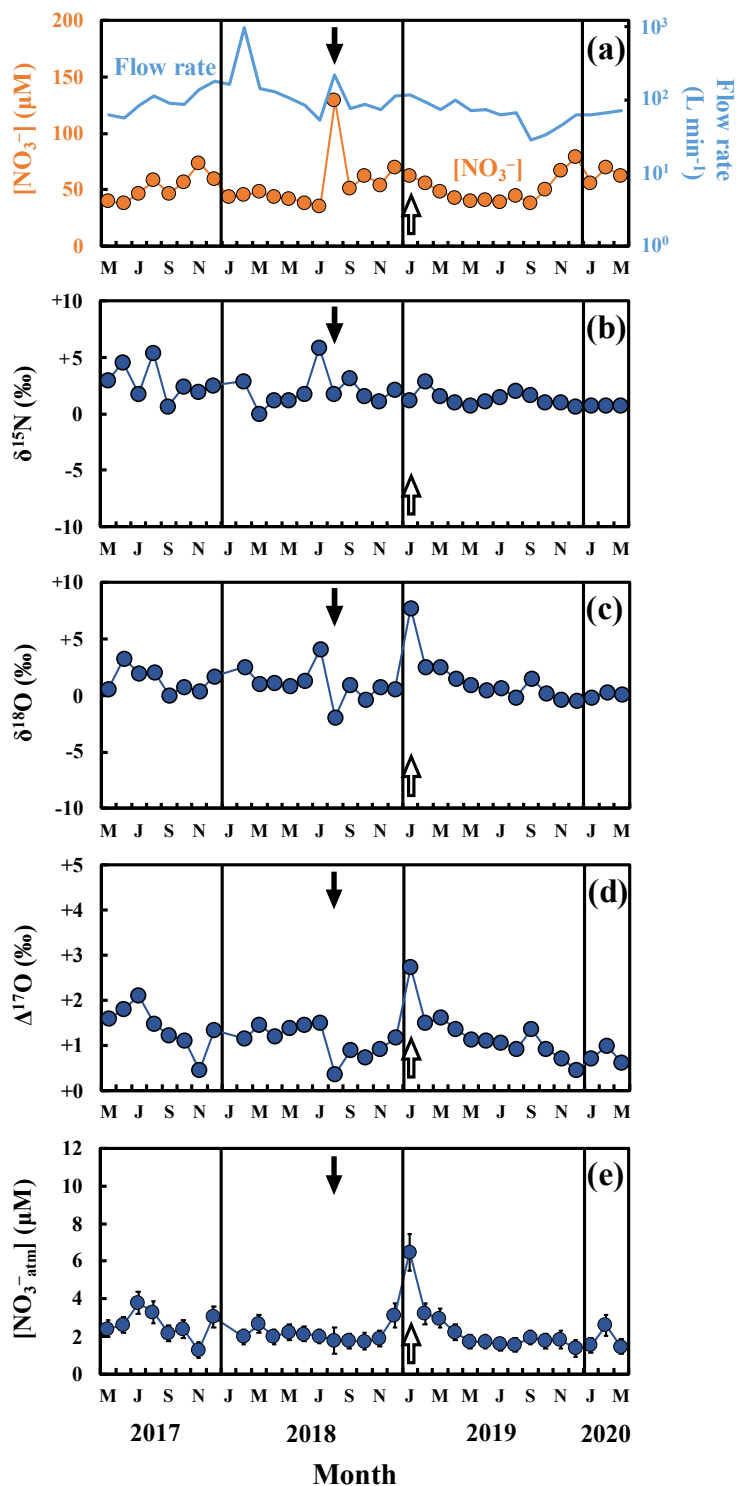
Figure 2. Temporal variations in the concentrations of nitrate (orange circles) and the

flow rates (blue line) in the stream water during the routine observation (a), together

with those of the values of $\delta^{15}N$ (b), $\delta^{18}O$ (c), $\Delta^{17}O$ (d) of nitrate, and the concentrations

271   of unprocessed atmospheric nitrate ($[NO_3^-{}_{atm}]$) (e) in the stream water (blue circles).

272   The black and white arrows in the figures indicate the sampling that took place on

273   2018/8/31 and 2019/1/31, respectively. The error bars smaller than the sizes of the

274   symbols are not presented.

275

276   3.2 Variation in response to the storm events

277   During the intensive observations made in response to the storm events, the

278   concentration of stream nitrate showed significant short-term variation, from 24.7 μM

279   to 122.6 μM, from 28.7 μM to 134.1 μM, and from 46.6 μM to 114.5 μM during the

280   storm events I, II, and III, respectively, with the minimum recorded just before the

281   beginning of each storm event and the maximum recorded when the flow rate was close

282   to the maximum within each storm event (Figs. 3 and S1). Similar increase in the

283   concentrations of stream nitrate in accordance with the increase in the flow rate during

284   storm events have been reported in many past studies (e.g. Burns et al.,2019; Chen et

285   al., 2020; Kamisako et al., 2008; Christopher et al., 2008). Especially, Kamisako et al.

286   (2008), who monitored temporal changes in the concentration of stream nitrate in the

287   same KJ catchment from 2003 to 2005 and found 11 nitrate increase events in

288   accordance with the increase in the flow rate, reported the largest concentration of

289   stream nitrate during the events to be 120 μM. The pattern and range of the short-term

290   variation of the stream nitrate concentration during the three storm events were also

291   consistent with the past study (Kamisako et al., 2008).

292   The stable isotopic compositions of stream nitrate during the three storm events also

293   showed significant temporal variation, from −0.1 ‰ to +2.5 ‰, from −0.5 ‰ to +3.0 ‰,

294   and from −0.1 ‰ to +3.5 ‰ for $\delta^{15}N$ (Figs. 3b, S1b, and S1g), from −3.4 ‰ to +3.1 ‰,

295   from −2.5 ‰ to +2.9 ‰, and from −2.3 ‰ to +2.1 ‰ for $\delta^{18}O$ (Figs. 3c, S1c, and S1h),

296   and from +0.3 ‰ to +1.6 ‰, from +0.3 ‰ to +1.4 ‰, and from +0.5 ‰ to +1.2 ‰ for

297      $\Delta^{17}O$ (Figs. 3d, S1d, and S1i), with minimum values observed when the concentration

298   of stream nitrate was at maximum and maximum values observed when the

299   concentration of stream nitrate was at a minimum.

300
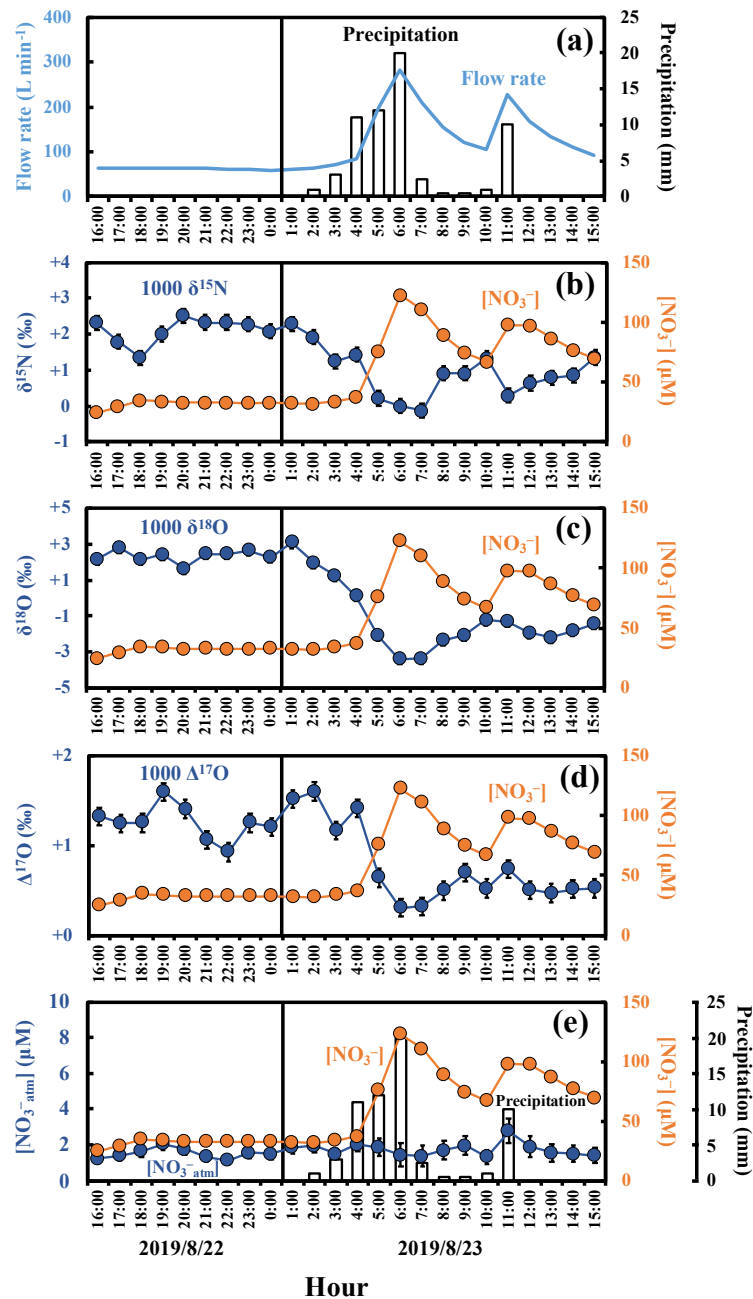
Figure. 3 Temporal variations in the amount of precipitation (bar chart) and flow rates of the stream water (blue line) during storm event I (a), together with those in the concentrations of nitrate (orange circles) (b-e), the values of $\delta^{15}N$ (b), $\delta^{18}O$ (c), $\Delta^{17}O$ (d) of nitrate, and $[NO_3^-{}_{atm}]$ (e) in the stream water (blue circles). The error bars smaller than the sizes of the symbols are not presented.

306

4 Discussion

4.1 Possible alterations to the concentration and isotopic compositions of stream nitrate

during the storage period in the automatic sampler used for the intensive observations

During the intensive observations, the stream water samples were stored in bottles of

the automatic sampler. The storage periods until filtration were ranged from 7 (storm

event I) to 12 days (storm event III) (Table 1). While the automatic sampler was

surrounded by ferns and the other understory vegetations to minimize the possible

alterations on the samples, progress of biogeochemical reactions such as nitrification,

denitrification, and assimilation could alter the concentration and isotopic compositions

($\delta^{15}N$, $\delta^{18}O$, and $\Delta^{17}O$) of stream nitrate during the storage period. Above all, possible

increase in soil water input into the stream water that is enriched with organic matters

during a storm event could enhance nitrification during the storage period and could

increase the concentration of nitrate in the stream water samples taken by using the

automatic sampler.

As a result, we discussed the possible alteration of the concentration and isotopic

compositions during the storage for the samples taken by using the automatic sampler

and concluded that the alterations during the storage in the automatic sampler were

minor in the samples. The details are described in Appendix A.

4.2 Primary source of nitrate increased during storm events

The striking feature of the observed short-term variation was that all the stable

327   isotopic compositions (δ^{15}N, δ^{18}O, and Δ^{17}O) varied in response to the variation in the

328   nitrate concentration throughout the three storm events (Figs. 3 and S1). The result

329   implied that the source of increased nitrate during the storm events were different from

330   that during the base flow period.

331   As a result, the stable isotopic compositions (δ^{15}N, δ^{18}O, and Δ^{17}O) of stream

332   nitrate were plotted as the functions of the reciprocal of the stream nitrate

333   concentration ($1/[NO_3^-]$) for each storm event (Fig. 4). All the stable isotopic

334   compositions of stream nitrate showed strong linear relationships ($R^2 > 0.5$; $p < 0.001$)

335   with the reciprocal of concentrations. The linear relationships strongly suggest mixing

336   between two endmembers with distinctively different isotopic signatures (e.g.

337   Keeling, 1958). The observed strong linear relationships not only in the Δ^{17}O of

338   stream nitrate (Figs. 4g, 4h, and 4i), which is stable during the progress of partial

339   removal reactions such as denitrification or assimilation, but also in the δ^{15}N and δ^{18}O

340   of stream nitrate (Figs. 4a-4f), which should be altered during the progress of the

341   partial removal reactions, also implied that the progress of denitrification or

342   assimilation in bottles of the automatic sampler during the storage period without

343   filtration were minor in the samples.

344   The nitrate-depleted endmember must be the source of stream nitrate during the

345   base flow period prior to each storm event. On the other hand, the nitrate-enriched

346   endmember represents the source of nitrate that was added during the storm events.

347 Atmospheric nitrate ($NO_3^-{}_{atm}$) dissolved in rainwater was one of the possible

348 sources of nitrate enriched during the storm events (Inamdar and Mitchell, 2006).

349 While the $NO_3^-{}_{atm}$ showed the $\delta^{18}O$ and $\Delta^{17}O$ values enriched in both ^{18}O and ^{17}O,

350 more than +55 ‰ and more than +18 ‰, respectively, during summer periods in

351 Japan (Tsunogai et al., 2016), the nitrate-enriched endmember showed the $\delta^{18}O$ and

352 $\Delta^{17}O$ values depleted in both ^{18}O and ^{17}O, less than +3.1 ‰ and +1.6 ‰, respectively,

353 during the storm events. During storm events, increase in $\delta^{18}O$ and/or $\Delta^{17}O$ have been

354 reported for stream nitrate eluted from forested catchments in past studies (Sebestyen

355 et al., 2019; Sabo et al., 2016; Buda and Dewalle. 2009). In KJ catchment, however,

356 we found significant decrease in both the $\delta^{18}O$ and $\Delta^{17}O$ of stream nitrate during

357 storm events. In addition, the concentrations of $NO_3^-{}_{atm}$ ($[NO_3^-{}_{atm}]$) showed little

358 temporal variations showing the concentrations of 1.6 ± 0.4 μM, 1.8 ± 0.4 μM, and

359 2.1 ± 0.4 μM during the storm events I, II, and III, respectively (Figs. 3e, S1e, and

360 S1j). In general, the $[NO_3^-{}_{atm}]$ in rainwater were much higher than those in stream

361 water (Nakagawa et al., 2018; Rose et al., 2015; Tsunogai et al., 2014). During the

362 storm events I, II, and III, however, the $[NO_3^-{}_{atm}]$ in stream water was almost constant

363 irrespective to the increase in precipitation (Figs. 3e, S1e, and S1j). Thus, we

364 conclude that the direct input of $[NO_3^-{}_{atm}]$ via rainwater into the stream through

365 overland flow during storm events can be negligible, at least in the KJ catchment.

366 Thus, we concluded that the $NO_3^-{}_{atm}$ should be the minor source of nitrate that

367 increased during the storm events.

368   Nakagawa et al. (2018) determined the temporal variations in the concentrations

369   (Fig. 5a) and isotopic compositions ($\delta^{15}N$, $\delta^{18}O$, and $\Delta^{17}O$) (Figs. 5b, 5c, and 5d) of

370   soil nitrate dissolved in soil water taken within the same catchment during 2013 to

371   2014, at the depths of 20 cm and 60 cm of the station SLS (SLS 20 and SLS 60,

372   respectively) and at the depth of 20 cm of the station SMS (SMS 20), where the

373   station SLS was located in the riparian zone of the stream and the station SMS was

374   about 20 m away from the stream and located in the upland zone (Fig. 1b). The

375   concentrations of soil nitrate showed significant seasonal variation, with the higher

376   concentration in summer and the lower concentration in winter (Fig. 5a). Both the

377    $\delta^{18}O$ and $\Delta^{17}O$ values also showed significant seasonal variation, with the minimum

378   in summer and the maximum in winter (Figs. 5c and d). To verify if the soil nitrate is

379   the source of the stream nitrate that was added to the stream during the storm events,

380   we also plotted soil nitrate at each site (SLS 20, SLS 60 and SMS 20) of the same

381   season in Fig. 4. Because our intensive observations on the storm events were done in

382   summer (from August to October), the average concentration and the average isotopic

383   composition during summer (from August to October) were calculated (Table 2) and

384   plotted in Fig. 4. The error bars of each soil nitrate denote the standard deviation (SD)

385   of each isotopic composition (n =5 for each). We found that the isotopic compositions

386   ($\delta^{15}N$, $\delta^{18}O$, and $\Delta^{17}O$) of soil nitrate in the riparian zone (SLS 20 and SLS 60; Table

387   2) were always plotted on the nitrate-enriched extension (lower $1/[NO_3^-]$ extension)

388   of the mixing line during the storm events I, II, and III (Fig. 4), while those of the soil

23

389   nitrate in the upland zone (SMS 20; Table 2) were somewhat deviated from the

390   nitrate-enriched extension of the mixing line, $\delta^{18}O$ especially (Figs. 4d, 4e, and 4f).

391   We conclude that the primary source of nitrate added during the storm events was the

392   soil nitrate in the riparian zone.

393   The "flushing hypothesis" has been proposed to explain the increase in stream

394   nitrate concentration in accordance with the increase in flow rate during storm events

395   (Creed et al., 1996; Hornberger et al., 1994). During the base flow periods, nitrate

396   accumulate in shallow, oxic soil layers due to the progress of nitrification. When

397   water level became higher during storm periods, concentration of stream nitrate

398   increased due to flushing of the soil nitrate accumulated in the shallow soil layers of

399   riparian zones into stream (Chen et al., 2020; Creed et al., 1996; Ocampo et al., 2006).

400   Our finding that the primary source of nitrate increased during the storm events was

401   the soil nitrate in the riparian zone is consistent with the "flushing hypothesis." We

402   conclude that the flushing of soil nitrate in the riparian zone into the stream due to

403   rising of both stream water and groundwater level was primarily responsible for the

404   increase in stream nitrate during the storm events (Fig. 6).

405   Within the whole dataset on the variation of the concentration of nitrate in the stream

406   determined by Kamisako et al. (2008), increases in the concentration of stream nitrate

407   to more than 20 µM in response to storm events were limited to the storm events that

408   occurred in the warm months, from June to November. As the concentrations of soil

409   nitrate in the riparian zone (SLS 20 and SLS 60) were much higher in the warm months

24

410   (734 µM ± 496 µM; from June to November) than in the cold months (156 ± 124 µM;

411   from December to May), such seasonal variation in the concentration of riparian soil

412   nitrate is consistent with the observed seasonality in the influence of storm events on

413   the stream nitrate concentration, where significant increase were limited to warm

414   months, whereas insignificant effects are observed during cold months.

415   The stream nitrate during storm events showed $\delta^{15}N$ values more depleted in ^{15}N than

416   those during the base flow periods (Figs. 3b, S1b, and S1g), probably due to the input

417   of riparian soil nitrate more depleted in ^{15}N. Compared with the $\delta^{15}N$ values of stream

418   nitrate taken during the base flow periods of routine observations when precipitation

419   was less than 1 mm/day (Fig. 2b; Table S1), the riparian soil nitrate (SLS 20 and SLS

420   60; Table 2) showed the $\delta^{15}N$ values around 3.5 ‰ lower. The trend and the extent of

421   the ^{15}N-depletion coincided well with those determined in the forested catchments in

422   past studies (Fang et al., 2015; Hattori et al., 2019). Fang et al. (2015), for instance,

423   reported significant differences between the $\delta^{15}N$ values of soil nitrate and those of

424   stream nitrate in six forested catchments in Japan and China, and proposed that the

425   kinetic fractionation due to the progress of denitrification during the elution of soil

426   nitrate into groundwater was responsible for the relative ^{15}N-enrichment in stream

427   nitrate compared with soil nitrate. As a result, the observed temporal decrease in the

428    $\delta^{15}N$ value of stream nitrate during storm events also supported that the flushing of soil

429   nitrate showing ^{15}N-depleted $\delta^{15}N$ values into the stream was responsible for the

430   elevated of nitrate concentrations during storm events.

431   As mentioned in section 3.1, we found significant increase in nitrate concentration

432   up to 129.3 µM on 2018/8/31 during our routine observation on the stream, when the

433   water was sampled in the middle of a heavy storm (48.0 mm/day; Table S1) with

434   significant increase in flow rate (from 53.4 L/min one month before to 216.9 L/min

435   during sampling), which the amount of precipitation on 2018/8/31 was the highest

436   within the whole routine observations (Table S1). The measured $\delta^{18}O$ and $\Delta^{17}O$ value

437   of the stream nitrate on 2018/8/31 (-1.9 ‰ and $+0.4$ ‰, respectively), showing

438   significantly smaller values than those during the other routine observation (Fig. 2c

439   and 2d), agreed well with those of the nitrate increase during the storm events I, II,

440   and III. Moreover, both the range of increase in stream nitrate concentration (129.3

441   µM) and the season of observation (August) also agreed well with those of the stream

442   nitrate increase during the three storm events. As a result, we conclude that the input

443   of soil nitrate accumulated in the riparian zone due to flushing was also responsible

444   for the significant increase in stream nitrate concentration we found on 2018/8/31

445   during the routine observation.
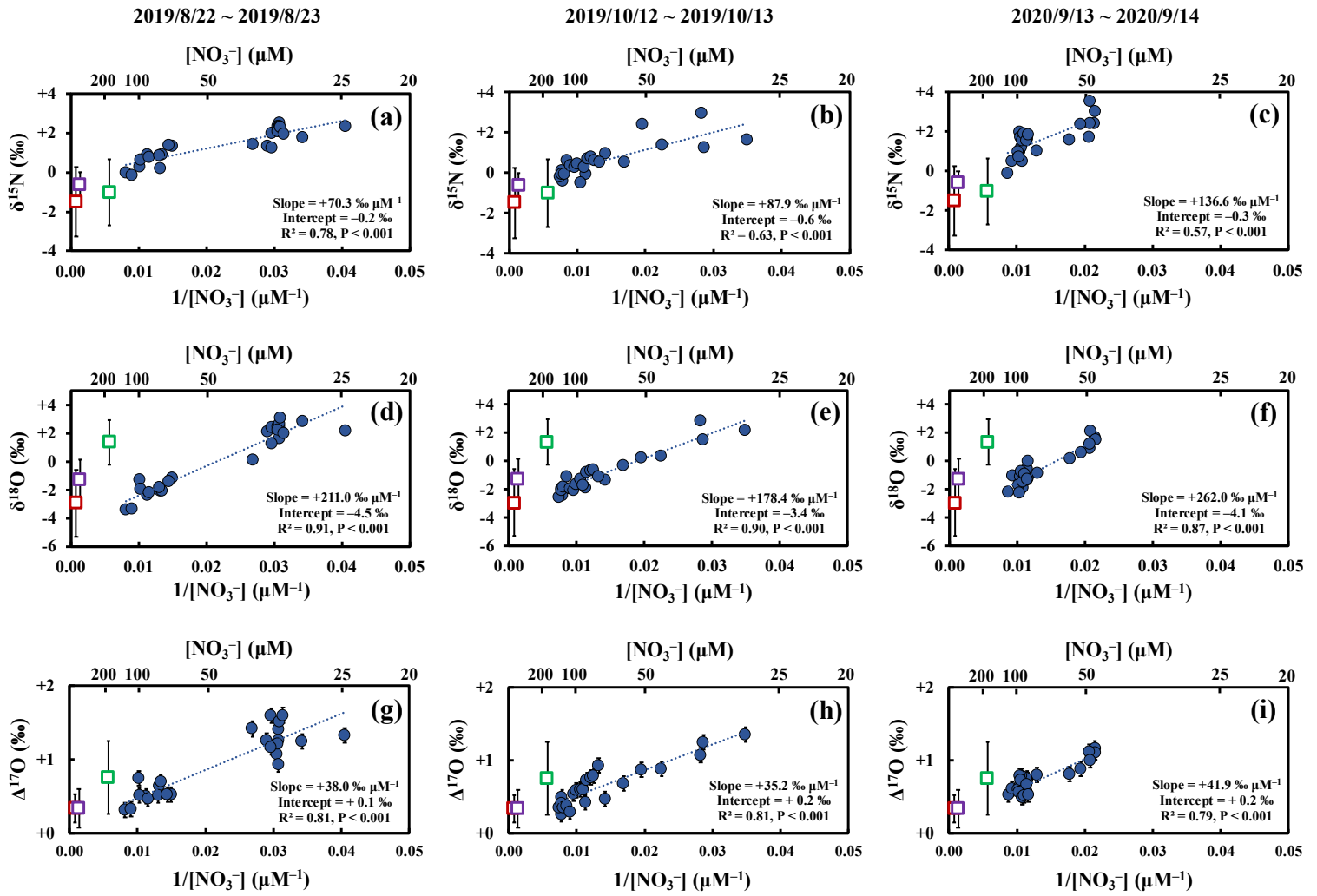
Figure 4. The $\delta^{15}N$ (a, b, and c), $\delta^{18}O$ (d, e, and f), and $\Delta^{17}O$ (g, h, and i) values of stream nitrate (blue circles) during storm events I, II, and III plotted as a function of the reciprocal of nitrate concentration $(1/[NO_3^-])$, together with those of soil nitrate at SLS 20 (red squares; riparian zone), SLS 60 (purple squares; riparian zone), and SMS 20 (green squares; upland zone) during August to October in 2013 and 2014. The error bars of each soil nitrate denote the standard deviation (SD) of each isotopic composition (n = 5 for each). The error bars smaller than the sizes of the symbols are not presented.
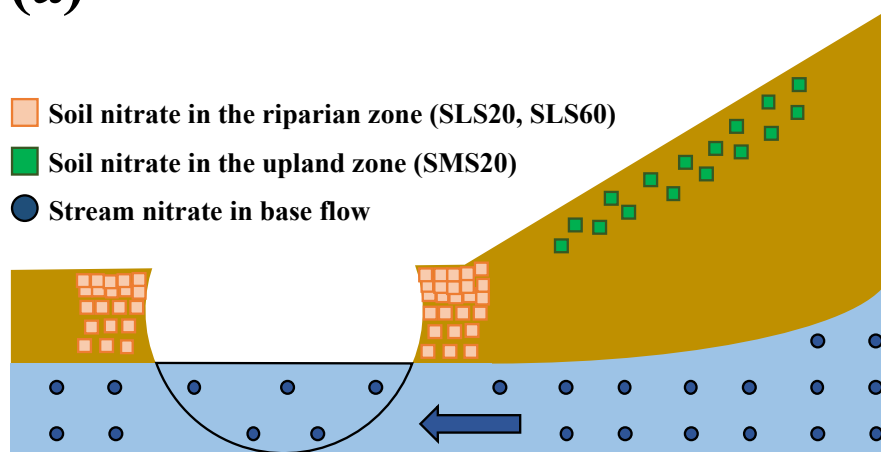
27
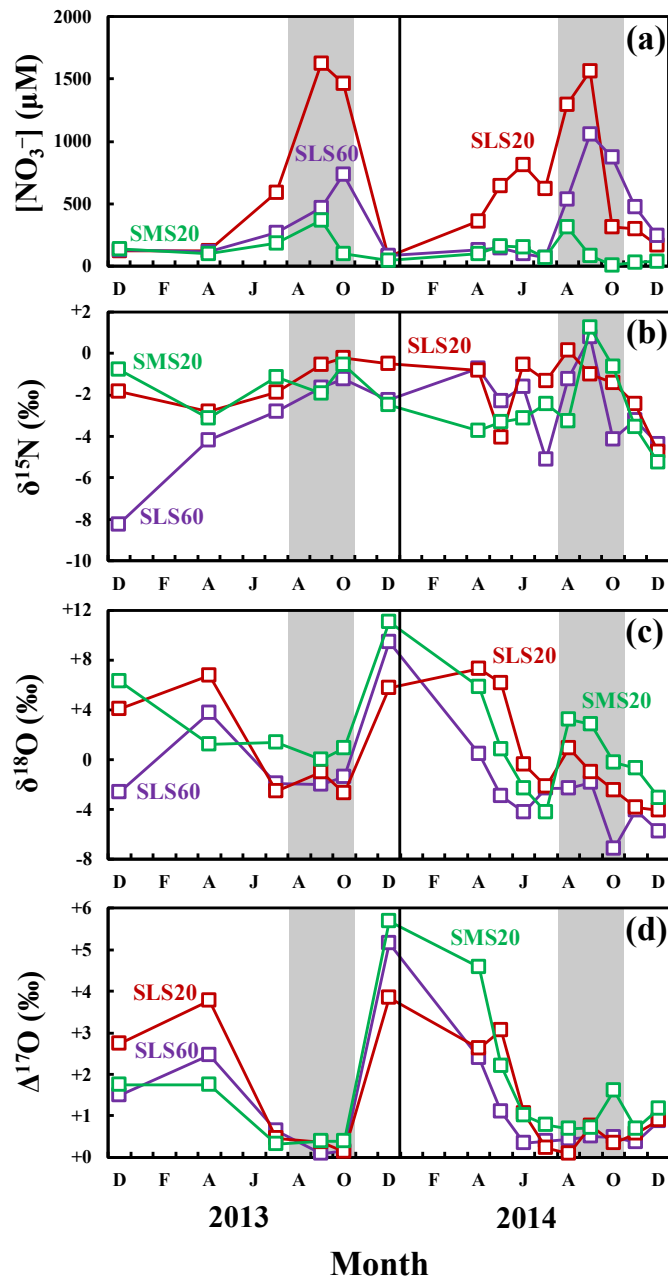
Figure 5. Seasonal variations in the concentrations of soil nitrate (a) at SLS 20 (red squares), SLS 60 (purple squares), and SMS20 (green squares), together with those in the values of $\delta^{15}N$ (b), $\delta^{18}O$ (c) and $\Delta^{17}O$ (d) of each soil nitrate during 2013 to 2014 (modified from Nakagawa et al., 2018). The periods used to estimate the isotopic compositions (from August to October) are presented in gray. The error bars were smaller than the sizes of the symbols.

Table 2. Concentrations and isotopic compositions (δ^{15}N, δ^{18}O, and Δ^{17}O) of soil nitrate

at SLS 20, SLS 60, and SMS 20 during August to October in 2013 and 2014

(recalculated from the data in Nakagawa et al., 2018).

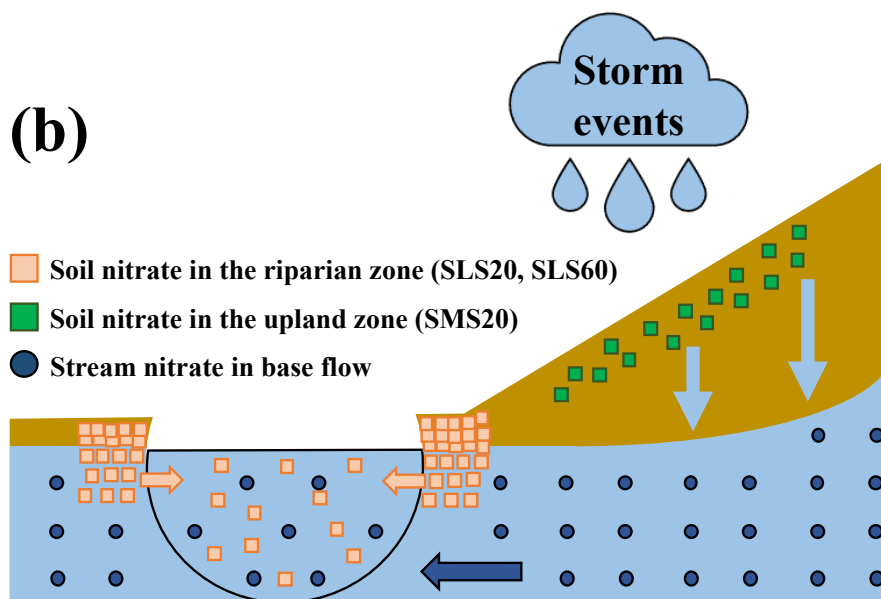|	SLS 20	SLS 60	SMS 20
NO_3^- (μM)	1254 ± 537	734 ± 241	176 ± 159
$1000\,\delta^{15}$N	-1.5 ± 1.8	-0.6 ± 0.6	-1.0 ± 1.7
$1000\,\delta^{18}$O	-2.9 ± 2.4	-1.3 ± 1.4	$+1.4 \pm 1.6$
$1000\,\Delta^{17}$O	$+0.3 \pm 0.2$	$+0.3 \pm 0.3$	$+0.8 \pm 0.5$

(a)

□ Soil nitrate in the riparian zone (SLS20, SLS60)
■ Soil nitrate in the upland zone (SMS20)
● Stream nitrate in base flow

(b)

Storm events

□ Soil nitrate in the riparian zone (SLS20, SLS60)
■ Soil nitrate in the upland zone (SMS20)
● Stream nitrate in base flow

467 **Figure 6.** Schematic diagram showing the elution of soil nitrate to the stream before

468 the storm events (a) and during the storm events (b). Soil nitrate in the riparian zone

469 and that in the upland zone are represented by the orange squares and green squares,

470 respectively, while stream nitrate during base flow is represented by the blue circles.

471

472 4.3 Variation in the concentration of $NO_3^-{}_{atm}$ during routine observation

473   The concentration of $NO_3^-{}_{atm}$ ($[NO_3^-{}_{atm}]$) showed little seasonal variation, from 1.3

474 µM to 3.8 µM during our routine observation in this study (Fig. 2e), except for the

475 extraordinarily large $[NO_3^-{}_{atm}]$ we found on 2019/1/31 (6.5 µM). Except for the

476 extraordinarily large $[NO_3^-{}_{atm}]$, the obtained $[NO_3^-{}_{atm}]$ corresponded well with those

477 determined in the past study done at the same catchment (Nakagawa et al., 2018). In

478 addition, they corresponded well with those of the temperate forested catchments

479 saturated in nitrogen, such as Fernow experimental Forest 3 (4.2 µM; Rose et al., 2015).

480   In this study, accumulation of snow up to 18 cm was observed at the KJ catchment

481 on 2019/1/27, while most of the accumulated snow had melted to a depth of 1 cm by

482 2019/1/30, just before the sampling on 2019/1/31. Furthermore, during the routine

483 observation period from 2017/5 to 2020/3, no other snow-melting events occurred

484 within 4 days prior to the day of sampling, except for the sampling on 2019/1/31.

485 Similar enhancement in the concentration of $NO_3^-{}_{atm}$, as well as the $\delta^{18}O$ and $\Delta^{17}O$ of

486 stream nitrate, in response to snow melting has been frequently observed in streams

487 worldwide (Ohte et al., 2004, 2010; Pellerin et al., 2012; Piatek et al., 2005; Rose et al.,

488 2015; Sabo et al., 2016; Tsunogai et al., 2014, 2016).

489   The flow rate, concentration of stream nitrate, and $\Delta^{17}O$ was 110.0 L/min, 70.0 μM,

490 and +1.17 ‰ on 2018/12/28, respectively, while 117.3 L/min, 62.4 μM, and +2.73 ‰

491 on 2019/1/31, respectively (Table S1). The $[NO_3{}^-_{atm}]$ in stream water was estimated to

492 be 3.1 μM on 2018/12/28 and 6.5 μM on 2019/1/31. Assuming that the $[NO_3{}^-_{atm}]$ in

493 snow melt was the same with the volume-weighted mean concentration of nitrate in

494 rainwater (41.0 μM) determined at Sado island in January (EANET, 2010, 2011;

495 Tsunogai et al., 2016), the increase in the flow rate ($\Delta F_{snowmelt}$) due to the mixing of

496 snow melt into the stream can be estimated to be 10.3 L/min, by using the mass balance

497 equation shown below:

498 $([NO_3{}^-_{atm}]_{2019/1/31} \times F_{2019/1/31} = [NO_3{}^-_{atm}]_{2018/12/28} \times F_{2018/12/28} + [NO_3{}^-_{atm}]_{snowmelt} \times$

499 $\Delta F_{snowmelt})$ (3)

500 where $[NO_3{}^-_{atm}]_{2018/12/28}$, $[NO_3{}^-_{atm}]_{2019/1/31}$, and $[NO_3{}^-_{atm}]_{snowmelt}$ denote the $[NO_3{}^-_{atm}]$ in

501 stream water on 2018/12/28, 2019/1/31, and that in snow melt water, respectively, and

502 $F_{2018/12/28}$, $F_{2019/1/31}$, and $\Delta F_{snowmelt}$ denote the flow rate of stream water on 2018/12/28,

503 2019/1/31, and the increase in the flow rate due to snow melt, respectively. Because the

504 estimated volume of melting snow water into the stream water (10.3 L/min) was

505 comparable with the observed increase in the flow rate from 2018/12/28 to 2019/1/31

506 (7.3 L/min), we concluded that the snow melting was responsible for the increase in

507 $\Delta^{17}O$ on 2019/1/31 and that the input of $NO_3{}^-_{atm}$ accumulated in the melted snow water,

508 showing $\delta^{18}O$ and $\Delta^{17}O$ values significantly higher than those in the stream, caused the

509   extraordinarily increase in $[NO_3^-{}_{atm}]$ on 2019/1/31. Except for the extraordinarily

510   increase in $[NO_3^-{}_{atm}]$ (n = 1), $[NO_3^-{}_{atm}]$ was stable at 2.2 ± 0.6 µM throughout the

511   routine observation (n = 33). We concluded that $[NO_3^-{}_{atm}]$ was generally stable in the

512   stream.

513

514   4.4 The impact of storm events on the index of the nitrogen saturation

515   The concentration of stream nitrate eluted from a forested catchment has been used

516   as an index to evaluate the stage of nitrogen saturation (Huang et al., 2020; Rose et al.,

517   2015; Stoddard, 1994). However, McHale et al. (2002) pointed out the problem in the

518   reliability of this index, because the number of storm events influenced the

519   concentration of nitrate eluted from forested stream significantly. That is, if we use the

520   concentration of stream nitrate sampled during the storm events to evaluate the stage of

521   nitrogen saturation in a forested catchment, the stage of nitrogen saturation might be

522   overestimated.

523   Nakagawa et al. (2018) have proposed the export flux of $NO_3^-{}_{atm}$ (M_{atm}) relative to

524   the deposition flux of $NO_3^-{}_{atm}$ (D_{atm}) can be an alternative, more robust index for

525   nitrogen saturation in temperate forested catchments, because the M_{atm}/D_{atm} ratio

526   directly reflect the demand on atmospheric nitrate deposited onto each forested

527   catchments as a whole, and thus reflect the nitrogen saturation in each forested

528   catchment. To estimate reliable M_{atm} in each forested catchment, we must obtain

529   reliable $[NO_3^-{}_{atm}]$ in the forested stream, including their temporal variation.

530   As already presented in section 4.2, we found that $[NO_3^-{}_{atm}]$ remained almost

531   constant irrespective to the significant variation in $[NO_3^-]$ during storm events (Figs.

532   3e, S1e, and S1j). The concentrations of atmospheric nitrate ($[NO_3^-{}_{atm}]$) in rainwater

533   were much higher than those in stream water. While the volume-weighted mean

534    $[NO_3^-{}_{atm}]$ in rainwater determined in Sado island from August to October, for example,

535   was 15.2 ± 8.4 μM (EANET, 2010, 2011; Tsunogai et al., 2016), that in the stream water

536   was 2.2 ± 0.6 μM in this study. As a result, the $[NO_3^-{}_{atm}]$ in stream water would increase,

537   if significant portion of rainwater was added directly into the stream water during the

538   storm events. The $[NO_3^-{}_{atm}]$ in stream water, however, was stable showing no

539   correlation with the amount of precipitation or the concentration of stream nitrate during

540   the storm events (Figs. 3e, S1e, and S1J). The $[NO_3^-{}_{atm}]$ remained almost constant as

541   well during the stream event on 2018/8/31 we found through the routine observation,

542   while $[NO_3^-]$ increased from 35.7 μM (1 month before) to 129.3 μM (Fig. 2e). As a

543   result, we concluded that the direct input of $NO_3^-{}_{atm}$ into the stream water was negligible

544   even during the storm events.

545   The observed $[NO_3^-{}_{atm}]$ showing almost constant values implies that the primary

546   source of $NO_3^-{}_{atm}$ in stream water during storm events was the $NO_3^-{}_{atm}$ stored in

547   groundwater, which is the same source as that during the base flow periods, rather than

548   the direct input of $NO_3^-{}_{atm}$ from rainwater. Because direct input of $NO_3^-{}_{atm}$ into stream

549   water was negligible during the storm events, the M_{atm}/D_{atm} ratio in each forested

550   catchment should be controlled by the metabolized processes (uptake or denitrification)

33

551 in each forested catchment subsequent to deposition, so that the M_{atm}/D_{atm} can correctly

552 reflect the total demand on $NO_3^-{}_{atm}$ in each forested catchment and thus the status of

553 nitrogen saturation. We conclude that the M_{atm}/D_{atm} ration can be a more robust index

554 to evaluate nitrogen saturation in forested catchments.

555

556 **5 Conclusions**

557   Temporal variations in the concentrations and stable isotopic compositions ($\delta^{15}N$,

558 $\delta^{18}O$, and $\Delta^{17}O$) of stream nitrate were determined during storm events to clarify the

559 source of stream nitrate increased during storm events. Because the stable isotopic

560 compositions of soil nitrate in riparian zone during summer agreed well with those of

561 the nitrate-enrich endmember of the stream nitrate increased during storm events, we

562 conclude that the soil nitrate in riparian zone was primarily responsible for the stream

563 nitrate increase during storm events. Additionally, the concentration of $NO_3^-{}_{atm}$ in the

564 stream was almost constant during the storm events, implied that the source of $NO_3^-{}_{atm}$

565 in stream water during storm events was the $NO_3^-{}_{atm}$ stored in groundwater. We

566 concluded that the number of storm events have little impact on M_{atm}/D_{atm} ratio, the

567 index of nitrogen saturation. In addition, the $\Delta^{17}O$ of nitrate can be applicable as the

568 tracer to clarify the source of nitrate.

569

570

571

Appendix A: Possible alterations to the concentration and isotopic compositions of stream nitrate during the storage period in the automatic sampler used for the intensive observations

During the intensive observations, the stream water samples were stored in bottles of the automatic sampler. The storage periods until filtration were ranged from 7 (storm event I) to 12 days (storm event III) (Table 1). While the automatic sampler was surrounded by ferns and the other understory vegetations to minimize the possible alterations on the samples, progress of biogeochemical reactions such as nitrification, denitrification, and assimilation could alter the concentration and isotopic compositions ($\delta^{15}N$, $\delta^{18}O$, and $\Delta^{17}O$) of stream nitrate during the storage period. Above all, possible increase in soil water input into the stream water that is enriched with organic matters during a storm event could enhance nitrification during the storage period and could increase the concentration of nitrate in the stream water samples taken by using the automatic sampler. Here, we discussed the possible alteration of the concentration and isotopic compositions during the storage for the samples taken by using the automatic sampler.

First, we compared the samples taken during the intensive observations using the automatic sampler with those taken during the routine observations. During the routine observations, the stream water samples were taken manually, transported to the laboratory within 1 h of each collection, passed through a membrane filter (pore size 0.45 μm), and stored in a refrigerator (4°C) until chemical analysis. As a result,

593   alterations should be minor in the samples taken through the routine observations.

594   When we compared the concentrations and isotopic compositions of stream nitrate

595   in the samples taken at the beginning of the intensive observation using the automatic

596   sampler with those in the routine observation nearby, they coincided well each other

597   (Table A1), implying that at least the progress of nitrification within the bottles of the

598   automatic sampler should be minor during the storage period because the concentration

599   of nitrate should increase, while the $\Delta^{17}O$ should decreased significantly during the

600   storage period if the progress of nitrification was active in the bottles of the intensive

601   observation.

602   In addition, a clear storm event was also observed during the routine observation on

603   2018/8/31 (Fig. 2; Table S1), so that we can compare the concentrations and isotopic

604   compositions of stream nitrate with those of intensive observations. During the routine

605   observation on 2018/8/31 done under a precipitation and flow rate of 48 mm/day and

606   216.9 L/min, respectively, we observed a significant increase in the concentration of

607   stream nitrate from 35.7 μM one month before to 129.3 μM (Fig. 2 and Table S1). In

608   accordance with the increase in the concentration, we found significant changes in the

609   isotopic compositions; from +5.9 ‰ to +1.8 ‰ for $\delta^{15}N$, from +4.1 ‰ to –1.9 ‰ for

610    $\delta^{18}O$, from +1.5 ‰ to +0.4 ‰ for $\Delta^{17}O$ (Fig. 2 and Table S1). The trend and the degree

611   of the variations in the concentration and the isotopic compositions on 2018/8/31 from

612   those on one month before were consistent with those of the intensive observation (Figs.

613   3 and S1). As a result, we concluded that the increase in the flow rate was responsible

614   for the observed increase in concentrations of stream nitrate during the storm events

615   and thus the microbial production of nitrate through nitrification during the storage had

616   little influence on the observed temporal changes in the concentrations and isotopic

617   compositions of nitrate in the stream water samples taken by using the automatic

618   sampler.

619   Kotlash and Chessman (1998) conducted storage experiments under various

620   conditions such as freezing, acidification, refrigeration, and room temperature to clarify

621   the changes in the concentrations of nitrogen compounds in stream water samples and

622   found little change in concentration of oxidized nitrogen ($NO_3^- + NO_2^-$) irrespective of

623   the treatments. To further verify the insignificant changes in the concentrations and

624   isotopic compositions of stream nitrate stored without treatments in the samples taken

625   by the automatic sampler, we also conducted the storage experiments by using a 100

626   mL of stream water taken at the KJ forested catchment on 2022/4/28 and stored in a

627   100 ml PP (polypropylene) bottle without treatments. Approximately 85 mL of the

628   stream water within the bottle was filtered using a GF/F filter paper (25 mm diameter)

629   and stored in a refrigerator (4°C) to determine original (initial) concentration and

630   isotopic compositions of nitrate. To simulate the stream water containing increased

631   suspended organic matters during the storm events, the GF/F filter paper was returned

632   to the 100 mL PP bottle which contained 15 mL of the stream water sample and left the

633   15 mL stream water under the room temperature (18.3°C) for 2 weeks together with the

634   suspended organic matters on the filter. The concentration and isotopic compositions of

635   the original stream nitrate (85 mL) and those being stored without filtration under the

636   room temperature for 2 weeks (15 mL) were analyzed by using the same method

637   presented in section 2.4. The concentration of nitrate in the stream water sample being

638   stored for 2 weeks without treatments coincided well with those in the original, showing

639   the difference in concentrations less than 10 % (Table A2). Besides, the differences in

640   the isotopic compositions from the original were also negligibly small (Table A2).

641   As a result, we concluded that the possible alteration in the concentration and isotopic

642   compositions of nitrate due to the progress of biogeochemical reactions such as

643   nitrification, denitrification, and assimilation during storage in the automatic sampler

644   used in the intensive observations was negligibly small.

645

646

647

648

649

650

651

652

653

654

655

656 **Table A1.** Comparison of both concentration and isotopic compositions ($\delta^{15}N$, $\delta^{18}O$,

657 and $\Delta^{17}O$) of stream nitrate between those taken at the beginning of intensive

658 observations using the automatic sampler and those taken manually on the days nearby

659 during routine observations.

	Type	Flow rate L/min	Precipitation mm/day	NO_3^- µM	$\delta^{15}N$ /10^3	$\delta^{18}O$ /10^3	$\Delta^{17}O$ /10^3
2019/7/31	routine	61.6	0.0	39.5	+1.55	+0.66	+1.06
2019/8/22 16:00	intensive	64.1	1.0	24.7	+2.32	+2.17	+1.33
2019/8/30	routine	66.0	13.0	44.9	+2.07	−0.13	+0.91
2019/9/30	routine	28.0	0.0	37.9	+1.65	+1.56	+1.36
2019/10/12 15:00	intensive	22.4	7.0	28.7	+1.61	+2.18	+1.35
2019/10/31	routine	32.6	0.0	50.4	+1.04	+0.19	+0.92
2020/9/13 11:00	intensive	111.0	0.0	46.6	+2.42	+1.74	+1.17
2020/9/30	routine	117.3	0.0	63.2	−	−	−

660 −:No samples were taken for isotopic analysis

661

662 Table A2. Comparison of both concentration and isotopic compositions ($\delta^{15}N$, $\delta^{18}O$,

663 and $\Delta^{17}O$) between original stream water sample and that being stored under the room

664 temperature for 2 weeks without treatments.

	NO_3^- µM	$\delta^{15}N$ /10^3	$\delta^{18}O$ /10^3	$\Delta^{17}O$ /10^3
Original	53.2	+0.90	+0.80	+1.05
Stored	49.5	+0.85	+0.90	+0.99

665

666 *Data availability.* All the primary data are presented in the Supplement. The other data

667 are available upon request to the corresponding author (Weitian Ding).

668

691

692 Reference

693 Aber, J. D., Nadelhoffer, K. J., Steudler, P. and Melillo, J. M.: Nitrogen Saturation in

694 Northern Forest Ecosystems, Bioscience, 39(6), 378–386, doi:10.2307/1311067,

695 1989.

696 Aguilera, R. and Melack, J. M.: Concentration-Discharge Responses to Storm Events

697 in Coastal California Watersheds, Water Resour. Res., 54(1), 407–424,

698 doi:10.1002/2017WR021578, 2018.

699 Alexander, B., Hastings, M. G., Allman, D. J., Dachs, J., Thornton, J. A. and

700 Kunasek, S. A.: Quantifying atmospheric nitrate formation pathways based on a

701 global model of the oxygen isotopic composition (δ^{17}O) of atmospheric nitrate,

702 Atmos. Chem. Phys., 9(14), 5043–5056, doi:10.5194/acp-9-5043-2009, 2009.

703 Buda, A. R. and DeWalle, D. R.: Dynamics of stream nitrate sources and flow

704 pathways during stormflows on urban, forest and agricultural watersheds in central

705 Pennsylvania, USA, Hydrol. Process., 23(23), 3292–3305,

706 doi:https://doi.org/10.1002/hyp.7423, 2009.

707 Burns, D. A. and Kendall, C.: Analysis of δ^{15}N and δ^{18}O to differentiate NO_3^- sources

708 in runoff at two watersheds in the Catskill Mountains of New York, Water Resour.

709 Res., 38(5), 91–912, doi:10.1029/2001wr000292, 2002.

710   Burns, D. A., Pellerin, B. A., Miller, M. P., Capel, P. D., Tesoriero, A. J. and Duncan,

711   J. M.: Monitoring the riverine pulse: Applying high-frequency nitrate data to advance

712   integrative understanding of biogeochemical and hydrological processes, Wiley

713   Interdiscip. Rev. Water, (October 2018), e1348, doi:10.1002/wat2.1348, 2019.

714   Chen, X., Tague, C. L., Melack, J. M. and Keller, A. A.: Sensitivity of nitrate

715   concentration-discharge patterns to soil nitrate distribution and drainage properties in

716   the vertical dimension, Hydrol. Process., 34(11), 2477–2493, doi:10.1002/hyp.13742,

717   2020.

718   Christopher, S. F., Mitchell, M. J., McHale, M. R., Boyer, E. W., Burns, D. A. and

719   Kendall, C.: Factors controlling nitrogen release from two forested catchments with

720   contrasting hydrochemical responses, Hydrol. Process., 22(1), 46–62,

721   doi:https://doi.org/10.1002/hyp.6632, 2008.

722   Creed, I. F., Band, L. E., Foster, N. W., Morrison, I. K., Nicolson, J. A., Semkin, R. S.

723   and Jeffries, D. S.: Regulation of nitrate-N release from temperate forests: A test of

724   the N flushing hypothesis, Water Resour. Res., 32(11), 3337–3354,

725   doi:10.1029/96WR02399, 1996.

726   Durka, W., Schulze, E., Gebauer, G. and Voerkeliust, S.: Effects of forest decline on

727   uptake and leaching of deposited nitrate determined from ^{15}N and ^{18}O measurements,

728   Nature, 372, 765−767, doi: https://doi.org/10.1038/372765a0, 1994.

729   EANET: Data Report 2010, Network center for EANET (Acid Deposition Monitoring

730   Network in East Asia), Nigata, Japan, 2011.

731   EANET: Data Report 2011, Network center for EANET (Acid Deposition Monitoring

732   Network in East Asia), Nigata, Japan, 2012.

733   Fang, Y., Koba, K., Makabe, A., Takahashi, C., Zhu, W., Hayashi, T., Hokari, A. A.,

734   Urakawa, R., Bai, E., Houlton, B. Z., Xi, D., Zhang, S., Matsushita, K., Tu, Y., Liu,

735   D., Zhu, F., Wang, Z., Zhou, G., Chen, D., Makita, T., Toda, H., Liu, X., Chen, Q.,

736   Zhang, D., Li, Y. and Yoh, M.: Microbial denitrification dominates nitrate losses from

737   forest ecosystems, Proc. Natl. Acad. Sci. U. S. A., 112(5), 1470–1474,

738   doi:10.1073/pnas.1416776112, 2015.

739   Galloway, J. N., Aber, J. D., Erisman, J. W., Seitzinger, S. P., Howarth, R. W.,

740   Cowling, E. B. and Cosby, B. J.: The nitrogen cascade, Bioscience, 53(4), 341–356,

741   doi:10.1641/0006-3568(2003)053[0341:TNC]2.0.CO;2, 2003.

742   Hattori, S., Nuñez Palma, Y., Itoh, Y., Kawasaki, M., Fujihara, Y., Takase, K. and

743   Yoshida, N.: Isotopic evidence for seasonality of microbial internal nitrogen cycles in

744   a temperate forested catchment with heavy snowfall, Sci. Total Environ., 690, 290–

745   299, doi:10.1016/j.scitotenv.2019.06.507, 2019.

746   Hirota, A., Tsunogai, U., Komatsu, D. D. and Nakagawa, F.: Simultaneous

747   determination of $\delta^{15}N$ and $\delta^{18}O$ of N_2O and $\delta^{13}C$ of CH_4 in nanomolar quantities from

748   a single water sample, Rapid Commun. Mass Spectrom., 24, 1085–1092,

749   doi:10.1002/rcm.4483, 2010.

750   Hornberger, G. M., Bencala, K. E. and McKnight, D. M.: Hydrological controls on

751   dissolved organic carbon during snowmelt in the Snake River near Montezuma,

752   Colorado, Biogeochemistry, 25(3), 147–165, doi:10.1007/BF00024390, 1994.

753   Huang, S., Wang, F., Elliott, E. M., Zhu, F., Zhu, W., Koba, K., Yu, Z., Hobbie, E.

754   A., Michalski, G., Kang, R., Wang, A., Zhu, J., Fu, S. and Fang, Y.: Multiyear

755   Measurements on $\Delta^{17}O$ of Stream Nitrate Indicate High Nitrate Production in a

756   Temperate Forest, Environ. Sci. Technol., 54(7), 4231–4239,

757   doi:10.1021/acs.est.9b07839, 2020.

758   Inamdar, S. P. and Mitchell, M. J.: Hydrologic and topographic controls on storm-

759   event exports of dissolved organic carbon (BOC) and nitrate across catchment scales,

760   Water Resour. Res., 42(3), 1–16, doi:10.1029/2005WR004212, 2006.

761   Inoue, T., Nakagawa, F., Shibata, H. and Tsunogai, U.: Vertical Changes in the Flux

762   of Atmospheric Nitrate From a Forest Canopy to the Surface Soil Based on $\Delta^{17}O$

763   Values, J. Geophys. Res. Biogeosciences, 126(4), 1–18, doi:10.1029/2020JG005876,

764   2021.

765   Kaiser, J., Hastings, M. G., Houlton, B. Z., Röckmann, T. and Sigman, D. M.: Triple

766   oxygen isotope analysis of nitrate using the denitrifier method and thermal

767   decomposition of N_2O, Anal. Chem., 79(2), 599–607, doi:10.1021/ac061022s, 2007.

768   Kamisako, M., Sase, H., Matsui, T., Suzuki, H., Takahashi, A., Oida, T., Nakata, M.,

769   Totsuka, T. and Ueda, H.: Seasonal and annual fluxes of inorganic constituents in a

770   small catchment of a Japanese cedar forest near the sea of Japan, Water. Air. Soil

771   Pollut., 195(1–4), 51–61, doi:10.1007/s11270-008-9726-8, 2008.

772   Keeling, D.: The concentration and isotopic abundances of atmospheric carbon

dioxide in rural areas, Geochim. Cosmochim. Acta, 13, 322–334,

doi:https://doi.org/10.1016/0016-7037(58)90033-4, 1958.

Kendall, C., Elliott, E. M. and Wankel, S. D.: Tracing Anthropogenic Inputs of

Nitrogen to Ecosystems, Stable Isot. Ecol. Environ. Sci. Second Ed., 375–449,

doi:10.1002/9780470691854.ch12, 2008.

Kotlash, A. R. and Chessman, B. C.: Effects of water sample preservation and storage

on nitrogen and phosphorus determinations: Implications for the use of automated

sampling equipment, Water Res., 32(12), 3731–3737, doi:10.1016/S0043-

1354(98)00145-6, 1998.

Komatsu, D. D., Ishimura, T., Nakagawa, F. and Tsunogai, U.: Determination of the

$^{15}N/^{14}N$, $^{17}O/^{16}O$, and $^{18}O/^{16}O$ ratios of nitrous oxide by using continuous-flow

isotope-ratio mass spectrometry Daisuke, Rapid Commun. Mass Spectrom., 22, 1587–

1596, doi:10.1002/rcm.3493, 2008.

Konno, U., Tsunogai, U., Komatsu, D. D., Daita, S., Nakagawa, F., Tsuda, A.,

Matsui, T., Eum, Y. J. and Suzuki, K.: Determination of total N2 fixation rates in the

ocean taking into account both the particulate and filtrate fractions, Biogeosciences,

7(8), 2369–2377, doi:10.5194/bg-7-2369-2010, 2010.

McHale, M. R., McDonnell, J. J., Mitchell, M. J. and Cirmo, C. P.: A field-based

study of soil water and groundwater nitrate release in an Adirondack forested

watershed, Water Resour. Res., 38(4), 2-1-2–16, doi:10.1029/2000wr000102, 2002.

McIlvin, M. R. and Altabet, M. A.: Chemical conversion of nitrate and nitrite to

794   nitrous oxide for nitrogen and oxygen isotopic analysis in freshwater and seawater,

795   Anal. Chem., 77(17), 5589–5595, doi:10.1021/ac050528s, 2005.

796   Michalski, G., Scott, Z., Kabiling, M. and Thiemens, M. H.: First measurements and

797   modeling of $\Delta^{17}O$ in atmospheric nitrate, Geophys. Res. Lett., 30(16), 3–6,

798   doi:10.1029/2003GL017015, 2003.

799   Michalski, G., Meixner, T., Fenn, M., Hernandez, L., Sirulnik, A., Allen, E. and

800   Thiemens, M.: Tracing Atmospheric Nitrate Deposition in a Complex Semiarid

801   Ecosystem Using $\Delta^{17}O$, Environ. Sci. Technol., 38(7), 2175–2181,

802   doi:10.1021/es034980+, 2004.

803   Mitchell, M. J., Iwatsubo, G., Ohrui, K. and Nakagawa, Y.: Nitrogen saturation in

804   Japanese forests: An evaluation, For. Ecol. Manage., 97(1), 39–51,

805   doi:10.1016/S0378-1127(97)00047-9, 1997.

806   Morin, S., Sander, R. and Savarino, J.: Simulation of the diurnal variations of the

807   oxygen isotope anomaly ($\Delta^{17}O$) of reactive atmospheric species, Atmos. Chem. Phys.,

808   11(8), 3653–3671, doi:10.5194/acp-11-3653-2011, 2011.

809   Nakagawa, F., Suzuki, A., Daita, S., Ohyama, T., Komatsu, D. D. and Tsunogai, U.:

810   Tracing atmospheric nitrate in groundwater using triple oxygen isotopes: Evaluation

811   based on bottled drinking water, Biogeosciences, 10(6), 3547–3558, doi:10.5194/bg-

812   10-3547-2013, 2013.

813   Nakagawa, F., Tsunogai, U., Obata, Y., Ando, K., Yamashita, N., Saito, T.,

814   Uchiyama, S., Morohashi, M. and Sase, H.: Export flux of unprocessed atmospheric

815   nitrate from temperate forested catchments: A possible new index for nitrogen

816   saturation, Biogeosciences, 15(22), 7025–7042, doi:10.5194/bg-15-7025-2018, 2018.

817   Nelson, D. M., Tsunogai, U., Ding, D., Ohyama, T., Komatsu, D. D., Nakagawa, F.,

818   Noguchi, I. and Yamaguchi, T.: Triple oxygen isotopes indicate urbanization affects

819   sources of nitrate in wet and dry atmospheric deposition, Atmos. Chem. Phys., 18(9),

820   6381–6392, doi:10.5194/acp-18-6381-2018, 2018.

821   Ocampo, C. J., Sivapalan, M. and Oldham, C.: Hydrological connectivity of upland-

822   riparian zones in agricultural catchments: Implications for runoff generation and

823   nitrate transport, J. Hydrol., 331(3–4), 643–658, doi:10.1016/j.jhydrol.2006.06.010,

824   2006.

825   Ohte, N., Sebestyen, S. D., Shanley, J. B., Doctor, D. H., Kendall, C., Wankel, S. D.

826   and Boyer, E. W.: Tracing sources of nitrate in snowmelt runoff using a high-

827   resolution isotopic technique, Geophys. Res. Lett., 31(21), 2–5,

828   doi:10.1029/2004GL020908, 2004.

829   Ohte, N., Tayasu, I., Kohzu, A., Yoshimizu, C., Osaka, K., Makabe, A., Koba, K.,

830   Yoshida, N. and Nagata, T.: Spatial distribution of nitrate sources of rivers in the lake

831   Biwa Watershed, Japan: Controlling factors revealed by nitrogen and oxygen isotope

832   values, Water Resour. Res., 46(7), 1–16, doi:10.1029/2009WR007871, 2010.

833   Paerl, H. W. and Huisman, J.: Climate change: A catalyst for global expansion of

834   harmful cyanobacterial blooms, Environ. Microbiol. Rep., 1(1), 27–37,

835   doi:10.1111/j.1758-2229.2008.00004.x, 2009.

Pellerin, B. A., Saraceno, J. F., Shanley, J. B., Sebestyen, S. D., Aiken, G. R.,

Wollheim, W. M. and Bergamaschi, B. A.: Taking the pulse of snowmelt: In situ

sensors reveal seasonal, event and diurnal patterns of nitrate and dissolved organic

matter variability in an upland forest stream, Biogeochemistry, 108(1–3), 183–198,

doi:10.1007/s10533-011-9589-8, 2012.

Peterjohn, W. T., Adams, M. B. and Gilliam, F. S.: Symptoms of nitrogen saturation

in two central Appalachian hardwood forest ecosystems, Biogeochemistry, 35(3),

507–522, doi:10.1007/BF02183038, 1996.

Piatek, K. B., Mitchell, M. J., Silva, S. R. and Kendall, C.: Sources of nitrate in

snowmelt discharge: Evidence from water chemistry and stable isotopes of nitrate,

Water. Air. Soil Pollut., 165(1–4), 13–35, doi:10.1007/s11270-005-4641-8, 2005.

Riha, K. M., Michalski, G., Gallo, E. L., Lohse, K. A., Brooks, P. D. and Meixner, T.:

High Atmospheric Nitrate Inputs and Nitrogen Turnover in Semi-arid Urban

Catchments, Ecosystems, 17(8), 1309–1325, doi:10.1007/s10021-014-9797-x, 2014.

Rose, L. A., Elliott, E. M. and Adams, M. B.: Triple Nitrate Isotopes Indicate

Differing Nitrate Source Contributions to Streams Across a Nitrogen Saturation

Gradient, Ecosystems, 18(7), 1209–1223, doi:10.1007/s10021-015-9891-8, 2015.

Sabo, R. D., Nelson, D. M. and Eshleman, K. N.: Episodic, seasonal, and annual

export of atmospheric and microbial nitrate from a temperate forest, Geophys. Res.

Lett., 43(2), 683–691, doi:10.1002/2015GL066758, 2016.

Sase, H., Takahashi, A., Sato, M., Kobayashi, H., Nakata, M. and Totsuka, T.:

857 Seasonal variation in the atmospheric deposition of inorganic constituents and canopy

858 interactions in a Japanese cedar forest, Environ. Pollut., 152(1), 1–10,

859 doi:10.1016/j.envpol.2007.06.023, 2008.

860 Sase, H., Saito, T., Takahashi, M., Morohashi, M., Yamashita, N., Inomata, Y.,

861 Ohizumi, T. and Nakata, M.: Transboundary air pollution reduction rapidly reflected

862 in stream water chemistry in forested catchment on the Sea of Japan coast in central

863 Japan, Atmos. Environ., 248(November 2020), 118223,

864 doi:10.1016/j.atmosenv.2021.118223, 2021.

865 Sebestyen, S. D., Ross, D. S., Shanley, J. B., Elliott, E. M., Kendall, C., Campbell, J.

866 L., Dail, D. B., Fernandez, I. J., Goodale, C. L., Lawrence, G. B., Lovett, G. M.,

867 McHale, P. J., Mitchell, M. J., Nelson, S. J., Shattuck, M. D., Wickman, T. R.,

868 Barnes, R. T., Bostic, J. T., Buda, A. R., Burns, D. A., Eshleman, K. N., Finlay, J. C.,

869 Nelson, D. M., Ohte, N., Pardo, L. H., Rose, L. A., Sabo, R. D., Schiff, S. L.,

870 Spoelstra, J. and Williard, K. W. J.: Unprocessed Atmospheric Nitrate in Waters of

871 the Northern Forest Region in the U.S. and Canada, Environ. Sci. Technol., 53(7),

872 3620–3633, doi:10.1021/acs.est.9b01276, 2019.

873 Stoddard, J. L.: Long-Term Changes in Watershed Retention of Nitrogen, , 223–284,

874 doi:10.1021/ba-1994-0237.ch008, 1994.

875 Tsunogai, U., Komatsu, D. D., Daita, S., Kazemi, G. A., Nakagawa, F., Noguchi, I.

876 and Zhang, J.: Tracing the fate of atmospheric nitrate deposited onto a forest

877 ecosystem in Eastern Asia using $\Delta^{17}O$, Atmos. Chem. Phys., 10(4), 1809–1820,

878   doi:10.5194/acp-10-1809-2010, 2010.

879   Tsunogai, U., Daita, S., Komatsu, D. D., Nakagawa, F. and Tanaka, A.: Quantifying

880   nitrate dynamics in an oligotrophic lake using $\Delta^{17}O$, Biogeosciences, 8(3), 687–702,

881   doi:10.5194/bg-8-687-2011, 2011.

882   Tsunogai, U., Komatsu, D. D., Ohyama, T., Suzuki, A., Nakagawa, F., Noguchi, I.,

883   Takagi, K. and Nomura, M.: Quantifying the effects of clear-cutting and strip-cutting

884   on nitrate dynamics in a forested watershed using triple oxygen isotopes as tracers, ,

885   (1), 5411–5424, doi:10.5194/bg-11-5411-2014, 2014.

886   Tsunogai, U., Miyauchi, T., Ohyama, T., Komatsu, D. D., Nakagawa, F., Obata, Y.,

887   Sato, K. and Ohizumi, T.: Accurate and precise quantification of atmospheric nitrate

888   in streams draining land of various uses by using triple oxygen isotopes as tracers,

889   Biogeosciences, 13(11), 3441–3459, doi:10.5194/bg-13-3441-2016, 2016.

890   Tsunogai, U., Miyauchi, T., Ohyama, T., Komatsu, D. D., Ito, M. and Nakagawa, F.:

891   Quantifying nitrate dynamics in a mesotrophic lake using triple oxygen isotopes as

892   tracers, Limnol. Oceanogr., 63, S458–S476, doi:10.1002/lno.10775, 2018.

893   Vitousek, P. M. and Howarth, R. W.: Nitrogen limitation on land and in the sea: How

894   can it occur?, Biogeochemistry, 13(2), 87–115, doi:10.1007/BF00002772, 1991.

895   Yamazaki, A., Watanabe, T. and Tsunogai, U.: Nitrogen isotopes of organic nitrogen

896   in reef coral skeletons as a proxy of tropical nutrient dynamics, Geophys. Res. Lett.,

897   38(19), 1–5, doi:10.1029/2011GL049053, 2011.